CHALMERS
UNIVERSITY OF TECHNOLOGY

Modelling and Contouring Error Bounded Control of a Biaxial Industrial Gantry Machine

2019 IEEE Conference on Control Technology and Applications (CCTA)
Hong Kong, China, August 19-21, 2019

Modelling and Contouring Error Bounded Control of a Biaxial Industrial Gantry Machine

Meng Yuan[1], Chris Manzie[2], Lu Gan[3], Malcolm Good[1] and Iman Shames[2]

Abstract— **Dual drive gantry machines are widely used in industry for manufacturing. However, the non-synchronised movement of the dual drive may lead to deterioration in contouring accuracy, and traditional control architectures commonly used in machining cannot explicitly bound the contouring error to meet a desired tolerance. In this paper, we propose a model predictive control architecture based on switched linear time invariant control-oriented models, that is able to guarantee a two-dimensional contouring tolerance in the presence of uncertainty arising from imperfect drive synchronisation. To develop the controller, we introduce a high-fidelity model for the dual drive gantry machine and identify its parameters using data from an industrial machine, and systematically reduce it to a control-oriented model. The performance and computational tractability of the proposed approach is demonstrated using high fidelity simulations.**

I. Introduction

XY positioning systems involve a manipulator moving over a two-dimension rectangular area for moving, marking, welding or cutting objects [1], [2]. Two hardware architectures are used to support the end effector, the cantilever beam (T-frame) and dual drive gantry (H-frame) systems. The former requires fewer parts and is lower cost, but suffers from relative structural flexibility and subsequent loss in performance compared with the dual drive systems, which typically have drives along each of the parallel axes [3]. This has seen more industrial interest in the dual drive systems for precision engineering applications such as laser cutting machines, which can have large operating envelopes.

However, difficulties in maintaining complete synchronisation in movement along the parallel axes can cause deformation in the beam and lead to deteriorated accuracy of the end effector. This non-synchronised behaviour may arise due to the different characteristics of the dual drives or the variational load distribution when loads moving along the gantry [4]. Consequently, some efforts have been devoted to modelling the dynamics of the dual drive gantry machine, e.g. [4], [5]. However, the movement of the end effector along the perpendicular axis as in [5], or other conditions such as lateral deformation in the crossbeam [4] which impact on accuracy of the end effector model relative to the real system are ignored.

The objective of controlling the end effector is generally stated for planar machining applications such as tracking a desired trajectory closely. Recently, various contouring control research works have been done on the gantry machine including [6], [7]. Such 'adaptive robust control' approaches generally rely on using an estimate of contouring error which is non-trivial to bound in practice. A sliding mode control method is utilised in [8] to minimise the synchronous and tracking error, however as in the other cases, a contouring error bound cannot be guaranteed. Ultimately, it is desirable to provide a guaranteed tolerance on the manufactured part.

In this paper, we firstly propose a physics-based model that possesses position-dependent structural coupling characteristics. The parameters of the proposed model are identified for a commercial industrial laser machine. To guarantee that the contour error is not violated during the entire process, we extend the single-axis bounded tracking error control methods in [9] to the two-axes scenario. The structure of the problem is exploited to partially decouple the controllers between axes and reduce the computational load in calculating the control outputs. Further simplification through the use of a switched linear time invariant (LTI) approach is undertaken to reduce the complexity of on-line calculations. The ability of the proposed controller to maintain a guaranteed tolerance is then demonstrated using a high-fidelity laser machine simulation.

II. System Modelling and Validation

A. Structural Configuration

A typical structure of the dual-drive gantry machine consists of two motors that separately sit on parallel linear slides carrying a crossbeam in the orthogonal direction. Generally, there is another drive on the gantry holding the end-effector head. Since intensive finite-element optimisation has been widely used for structural design of industrial machines, the structural parts generally have more rigidity than the joints. Such machines can be successfully modelled with rigid elements connected by flexible joints [10]. In order to capture the characteristics of systems with limited stiffness, we propose a model with linear and torsional springs to represent the flexible joint that links the crossbeam with the longitudinal motor as shown in Fig. 1. This schematic figure shows the behaviour of the system when dual drive is in synchronised (dot grey line) and non-synchronised (solid black line) conditions. In order to allow the lateral deformation in Y direction, linear springs that link the Y-axis motors and linear guide are introduced. The two linear

[1]Meng Yuan and Malcolm Good are with the Department of Mechanical Engineering, The University of Melbourne, Parkville, VIC 3010, Australia. yuanm3@student.unimelb.edu.au, mcgood@unimelb.edu.au

[2]Chris Manzie and Iman Shames are with the Department of Electrical and Electronic Engineering, The University of Melbourne, Parkville, VIC 3010, Australia. manziec@unimelb.edu.au, iman.shames@unimelb.edu.au

[3]Lu Gan is with ANCA Motion, Bayswater North, Victoria 3153, Australia. lu.gan@ancamotion.com

978-1-7281-2767-5/19/$31.00 ©2019 IEEE

springs with spring constant k_s are assumed symmetrically located at the vertical centre of the two sides of each Y-axis motors.

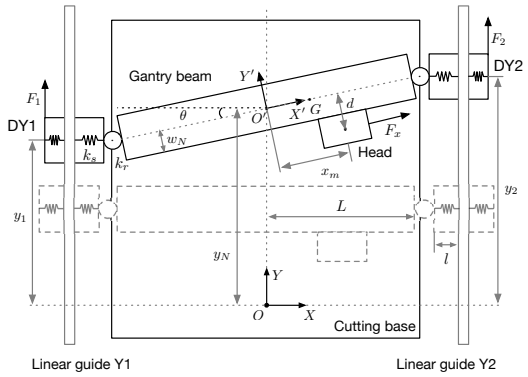

Fig. 1. Schematic of moving gantry machine with Y-axis movement dis-synchronisation.

In the schematic of the gantry machine, OXY is the fixed inertial coordinate frame with origin O located in the middle point between the two linear guides and Y-axis parallel to the linear guides. Let O' be the centre of mass (CoM) of the crossbeam. The half-length of the crossbeam and motor are L and l respectively. The half-width of the beam is w_N. The dual drives on Y axis are denoted as $DY1$ and $DY2$ respectively. Here, $O'X'Y'$ is a moving coordinate system with the X'-axis paralleling the lateral direction of the beam.

When the movements of the two Y-axis drives are not synchronised perfectly, the angle formed between the X and X' axes is θ. The moving distance of the X-axis head respect to $O'X'Y'$ frame is x_m which can be directly measured by the linear encoder on the gantry. Let d denote the projection of the distance between the head and beam mass centre in the Y' direction. With the inclusion of the moving head and some carriage blocks, the mass centre G of the entire rigid parts should be different from the O'. However, considering the mass of the head is relatively small compared to the total mass of other parts, the mass centre G is close enough to the O'. We assume the gantry beam rotates around O' in the later analysis when a Y-axis offset occurs.

Finally, let y_1, y_2 be the position of the Y-axis motors along the respective guides, which can be measured by the linear encoders.

B. Lagrangian-based System Modelling

If it is assumed that the rotation angle of the gantry is small and the beam is rigid, the angle of rotation and position of CoM for the gantry beam can be approximated by $\theta = (y_2 - y_1)/2L$ and $y_N = (y_1 + y_2)/2$. Linear springs are included to support some degree of misalignment between $DY1$ and $DY2$, although translational dynamics are neglected in the modelling. The planar movement dynamics can be described by the generalised coordinates x_m, y_N and θ.

Based on these generalised coordinates, the CoM positions of Y-axis drives, gantry and end effector head are respectively defined as:

$$\begin{aligned}
P_1 &= (x_1, y_1) = (-L\cos\theta - l, y_N - L\sin\theta),\\
P_2 &= (x_2, y_2) = (L\cos\theta + l, y_N + L\sin\theta),\\
P_N &= (0, y_N),\\
P_e &= (x_m\cos\theta + d\sin\theta, y_N + x_m\sin\theta - d\cos\theta).
\end{aligned}$$

The velocity of the four separate objects, namely two dual drives, gantry and end effector head, are denoted as V_1, V_2, V_N and V_e with value:

$$V_1 = \begin{bmatrix} L\sin\theta\dot{\theta} \\ \dot{y}_N - L\cos\theta\dot{\theta} \end{bmatrix}, V_2 = \begin{bmatrix} -L\sin\theta\dot{\theta} \\ \dot{y}_N + L\cos\theta\dot{\theta} \end{bmatrix},$$

$$V_N = \begin{bmatrix} 0 \\ \dot{y}_N \end{bmatrix}, V_e = \begin{bmatrix} \Gamma\cos\theta - x_m\sin\theta\dot{\theta} \\ \dot{y}_N + \Gamma\sin\theta + x_m\cos\theta\dot{\theta} \end{bmatrix}, \quad (1)$$

where $\Gamma = \dot{x}_m + d\dot{\theta}$. Let M_1, M_2, M_e and M_n denote the mass of the drive $DY1$, drive $DY2$, X-axis head drive, and the gantry respectively. Since the gantry and end-effector are two distinct rigid bodies, only the rotary kinetic energy of the gantry is calculated. Let I_N denote the moment of inertia of the gantry corresponding to the central point O' as:

$$I_N = \frac{1}{12}M_n\left((2L)^2 + (2w_N)^2\right). \quad (2)$$

The moment of inertia of the end effector head about its centre of mass is assumed negligible. The total kinetic energy is then calculated as

$$\begin{aligned}
\mathcal{K} =& \frac{1}{2}M_1V_1^TV_1 + \frac{1}{2}M_2V_2^TV_2 + \frac{1}{2}M_nV_N^TV_N\\
&+ \frac{1}{2}M_eV_e^TV_e + \frac{1}{2}I_N\dot{\theta}^2. \quad (3)
\end{aligned}$$

The total potential energy stored in linear and torsional springs is $\mathcal{P} = k_r\theta^2 + k_sL^2\left(1-\cos\theta\right)^2$. The Lagrangian, $\mathcal{L} = \mathcal{K} - \mathcal{P}$, allows the dynamic equations for this three degree-of-freedom system with generalised coordinates $q_j = \{x_m, y_N, \theta\}$, $j = 1, 2, 3$ to be calculated from the Lagrange equation $\frac{d}{dt}\left(\frac{\partial\mathcal{L}}{\partial\dot{q}_j}\right) - \frac{\partial\mathcal{L}}{\partial q_j} = Q_{q_j}$.

The external generalised forces Q_{q_j} are computed based on kinematic approach:

$$Q_{x_m} = k_xi_x - b_x\dot{x}_m, \quad (4)$$

$$Q_{y_N} = k_y(i_1 + i_2) - b_y(\dot{y}_1 + \dot{y}_2), \quad (5)$$

$$Q_\theta = \left(k_y(i_2 - i_1) - b_y(\dot{y}_2 - \dot{y}_1)\right)L\cos\theta, \quad (6)$$

where k_x, k_y are the force constant of the X, Y-axis motors; i_x, i_1, i_2 are the current inputs of the end effector motor, and drives $DY1$ and $DY2$ respectively; b_x, b_y are the viscous friction coefficient of gantry and linear guides, where the viscous coefficients on $Y1$ and $Y2$ are assumed identical.

The governing equations of the gantry mechanism are given by (7), (8) and (9), where $M_t = M_1 + M_2 + M_e + M_n$ is the total mass of the system; $M_d \triangleq M_1 - M_2$ is the mass difference. Unlike existing models, the governing equations are able to capture the position dependent structural variation when the head motor moves along the gantry beam.

$$M_e(-x_m\dot{\theta}^2 + \ddot{x}_m + d\ddot{\theta} + \ddot{y}_N \sin\theta) = Q_{x_m} \tag{7}$$

$$M_e \sin\theta \ddot{x}_m + M_t\ddot{y}_N + (M_e d\sin\theta - M_d L\cos\theta + M_e x_m \cos\theta)\ddot{\theta} + M_e(-x_m \sin\theta\dot{\theta}^2 + 2\dot{x}_m\cos\theta\dot{\theta} + d\dot{\theta}^2\cos\theta) + M_d L\dot{\theta}^2\sin\theta = Q_{y_N} \tag{8}$$

$$M_e d\ddot{x}_m + (M_e d\sin\theta - M_d L\cos\theta + M_e x_m\cos\theta)\ddot{y}_N + \left(L^2(M_1+M_2) + \frac{M_n(L^2+w_N^2)}{3} + M_e\left(d^2+x_m^2\right)\right)\ddot{\theta} + 2k_r\theta + 2L^2k_s\sin\theta(1-\cos\theta) + 2M_e\dot{\theta}\dot{x}_m x_m = Q_\theta \tag{9}$$

C. Control Oriented Modelling

The dynamics equation (7) can be reformulated as (10) by lumping all terms involving y_N, θ into a disturbance term:

$$\ddot{x}_m + \frac{b_x}{M_e}\dot{x}_m = \frac{k_x}{M_e}i_x + F_{dx}, \tag{10}$$

where the disturbance term is $F_{dx} \triangleq x_m\dot{\theta}^2 - d\ddot{\theta} - \ddot{y}_N\sin\theta$. To develop an approximate model of Y-axis without dependence on the dynamics of x_m, the (8) and (9) are approximated at different operating point $\bar{x}_m$ and rearranged as follows by applying a small angle approximation:

$$M_t\ddot{y}_N + 2b_y\dot{y}_N + M_e\bar{x}_m\ddot{\theta} = k_y(i_1+i_2) + F_{d1}, \tag{11}$$

$$M_e\bar{x}_m\ddot{y}_N + J\ddot{\theta} + 2b_yL^2\dot{\theta} + 2k_r\theta = k_yL(i_2-i_1) + F_{d2}, \tag{12}$$

where M_d is assumed to be zero; $J(\bar{x}_m) = J_0 + M_e\bar{x}_m^2$ is the total moment of inertia which depends on value of $\bar{x}_m$, and $J_0 = L^2(M_1+M_2) + \frac{M_n(L^2+w_N^2)}{3} + M_e d^2$; the disturbance force are $F_{d1} = M_e(\bar{x}_m\theta\dot{\theta}^2 - \theta\ddot{x}_m - d\theta\ddot{\theta} - 2\dot{x}_m\dot{\theta} - d\dot{\theta}^2)$ and $F_{d2} = -M_e(2\dot{\theta}\dot{x}_m\bar{x}_m + d\theta\ddot{y}_N + d\ddot{x}_m)$.

Multiple linearisation for different $\bar{x}_m$ is undertaken to reduce the model mismatch, leading to a switched LTI model for these axes.

III. System Identification and Model Validation

To parameterise the proposed model, data was collected from a commercial laser machine with 1.5 m beam length and 3 m moving distance in Y-axis with 0.1 μm measurement resolution.

To simplify the system identification, the terms $M_e\bar{x}_m\ddot{\theta}$ and $M_e\bar{x}_m\ddot{y}_N$ arising after applying a small angle approximation to (8) and (9) are neglected and considered as plant-model mismatch. The full order model is then approximated by the following dynamic equations for y_1 and y_2:

$$M_t\left(\frac{\ddot{y}_1+\ddot{y}_2}{2}\right) + b_y(\dot{y}_1+\dot{y}_2) = k_y(i_1+i_2) \tag{13}$$

$$J\frac{\ddot{y}_2-\ddot{y}_1}{2L} + b_yL(\dot{y}_2-\dot{y}_1) + k_r\frac{y_2-y_1}{L} = k_yL(i_2-i_1) \tag{14}$$

Noting J has $\bar{x}_m$ dependency, the approximated transfer function from current i_1 to the drive velocity $\dot{y}_1$ is:

$$G_{iv1}(s) = \frac{k_y\left(\left(J+L^2M_t\right)s^2 + 4L^2b_ys + 2k_r\right)}{(M_ts+2b_y)\left(Js^2+2L^2b_ys+2k_r\right)} \tag{15}$$

Several of these parameters can be identified from the machine data sheet (e.g. the force constants, k_x and k_y) while the remainder (e.g. J_0, M_t, b_y, k_r) must be identified from the frequency response of collected data. During the data collection, the Y-axis motors are excited with a 4 A peak amplitude chirp-signal current when X-axis motor is held constant at $\bar{x}_m = 0$ m and $\bar{x}_m = -0.66$ m.

The experimental and modelled frequency responses are shown in Fig. 2 and Fig. 3. The physical system exhibits a change in anti-resonance frequency from approximately 47 Hz to 45 Hz as the X-axis motor is moved from 0 to 66 cm along the gantry beam, exhibiting a state-dependence of this motor on the resulting dynamics. The modelled system is able to capture this dependence and also exhibits a similar magnitude shift in anti-resonance frequency.

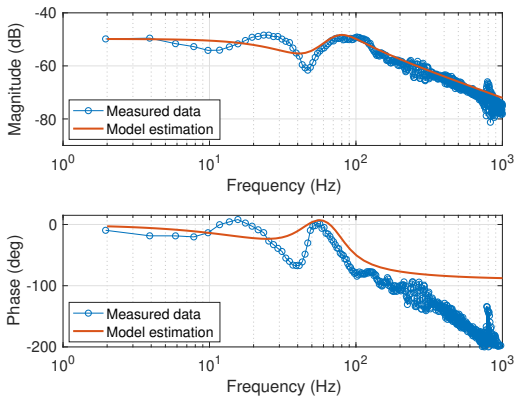

Fig. 2. Bode plot from drive current to velocity when laser head is located at $\bar{x}_m = 0$ m.

IV. Proposed Predictive Control Structure

For the type of two-axes contouring problems commonly seen industrially, the reference trajectory is time stamped and is therefore different to other path following problems. In this section we will present a model predictive control (MPC) tracking algorithm to address this problem with bounded contouring error.

A. Bounded Contouring Error and Bounded Tracking Error

As shown in Fig. 4, for a location of the end effector, $(x_e(k), y_e(k))$ at time k, let $(x^c(k), y^c(k))$ be the closest projection of end-effector onto the desired path. The reference trajectory will have a desired location $\left(x^d(k), y^d(k)\right)$,

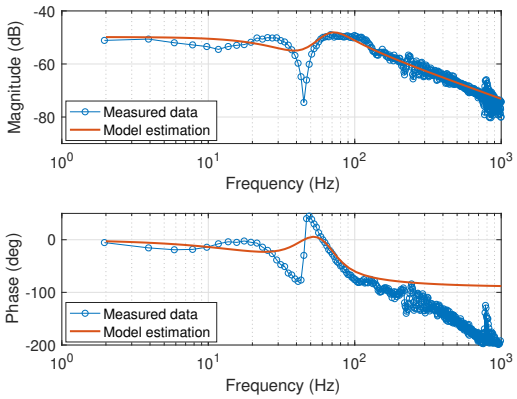

Fig. 3. Bode plot from drive current to velocity when laser head is located at $\bar{x}_m = -0.66$ m.

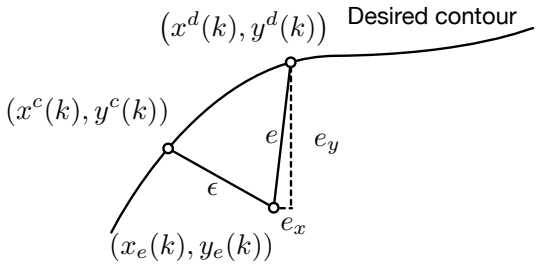

Fig. 4. Bounded tracking error leads bounded contouring error.

and thus the contouring error is ϵ and distance between actual position and desired position is e.

Lemma 1. Given a desired contouring error bound ϵ_c, the bounded contouring error $\|\epsilon\|_\infty \leq \epsilon_c$ can be guaranteed by bounding the tracking error of X and Y axes as $\|e_x\|_\infty + \|e_y\|_\infty \leq \epsilon_c$.

Proof: Since x^c is the closest point from the actual end effector position, we have $|\epsilon(k)| \leq |e(k)|, \forall k$. Based on the triangle inequality, we have $|e(k)| \leq |e_x(k)| + |e_y(k)|$. Then the following inequalities hold: $|\epsilon(k)| \leq |e(k)| \leq |e_x(k)| + |e_y(k)| \leq \epsilon_c$. ■

From Lemma 1, the control objective can be restated as ensuring $\|e_x\|_\infty \leq \epsilon_x$ and $\|e_y\| \leq \epsilon_y$, where $\epsilon_x + \epsilon_y = \epsilon_c$.

Because the X-axis tracking error in the control oriented model is $e_x = x^d - x_e = x^d - x_m - d\theta$, the following remark is provided to show how to ensure $\|e_x\|_\infty \leq \epsilon_x$ based on the X-axis dynamics and reference trajectory.

Remark 1: Consider a desired X-axis tracking error bound, ϵ_x that the system is initialised within, and set the rotation angle constraint as $|\theta| \leq \theta_{max} \leq \epsilon_x/d$. If the designed X-axis controller can guarantee $|x^d(k) - x_m(k)| \leq \epsilon_x - d\theta_{max}, \forall k$, the bounded tracking error can be guaranteed, i.e. $\|e_x\|_\infty \leq \epsilon_x$. Note that the RCI set calculation in this instance potentially introduces an asymmetry between the X- and Y- axes error bounds due to the $d\theta_{max}$ tightening of ϵ_x. This is an artefact of decoupling the axes controller in the proposed approach.

B. Error Bounded Model Predictive Control Formulation

An tracking error bounded control method for a single axis machine described as a LTI system with disturbance has been proposed in [9]. We now extend this work to allow bounds to be imposed on contouring error in biaxial systems.

The reference trajectory for the end-effector position is generated off-line and with specified position, velocity and acceleration constraints. In keeping with standard approaches, we assume an LTI system as the reference model for trajectory generation:

$$r^+ = A_r r + B_r u_r, \tag{16}$$

where $r \in \mathbb{R}^2$, $u_r \in \mathbb{R}$ are the state and input of the reference model. The matrices A_r and B_r are given with reference sampling time T_r as:

$$A_r = \begin{bmatrix} 1 & T_r \\ 0 & 1 \end{bmatrix}, B_r = \begin{bmatrix} 0 \\ T_r \end{bmatrix}.$$

For X-axis reference, r and u_r can be $r_x \triangleq \begin{bmatrix} x^d & v_x^d \end{bmatrix}^T$, $u_r \triangleq a_x$ where x^d and v_x^d are the desired position and velocity, a_x is the desired acceleration. The same model (16) can be used to describe the evolution of Y axis reference as well when states $r_y \triangleq \begin{bmatrix} y^d & v_y^d \end{bmatrix}^T$ represents the Y-axis desired position, velocity and $u_r \triangleq a_y$ is the acceleration. The reference trajectory generated with (16) is considered to satisfy constraints of the form:

$$\begin{bmatrix} -\bar{x} \\ -\bar{v}_x \end{bmatrix} \leq r_x \leq \begin{bmatrix} \bar{x} \\ \bar{v}_x \end{bmatrix}, -\bar{a}_x \leq a_x \leq \bar{a}_x, \tag{17}$$

$$\begin{bmatrix} -\bar{y} \\ -\bar{v}_y \end{bmatrix} \leq r_y \leq \begin{bmatrix} \bar{y} \\ \bar{v}_y \end{bmatrix}, -\bar{a}_y \leq a_y \leq \bar{a}_y. \tag{18}$$

The discrete-time state space models for the X- and Y-axis can be derived from (10), (11) and (12) with given sampling time T_s as

$$\xi_x^+ = A_x \xi_x + B_x i_x + E_x F_{dx}, \tag{19}$$

$$\xi_y^+ = A_y(\bar{x}_m)\xi_y + B_y(\bar{x}_m) i_y + E_y(\bar{x}_m) F_{dy}, \tag{20}$$

where $\xi_x \triangleq \begin{bmatrix} x_m & \dot{x}_m \end{bmatrix}^T$, $\xi_y \triangleq \begin{bmatrix} y_N & \dot{y}_N & \theta & \dot{\theta} \end{bmatrix}^T$ are the states, i_x, $i_y = \begin{bmatrix} i_1 & i_2 \end{bmatrix}^T$ are the inputs. The system coefficient matrix of (19) and (20) and disturbance vector F_{dy} can be inferred from (11) and (12), but are not provided explicitly here due to the space limitation.

The states and inputs of the system are required to remain within bounded constraints, i.e.:

$$\xi_x \in \mathcal{X}_m \subseteq \mathbb{R}^2, \xi_y \in \mathcal{X}_y \subseteq \mathbb{R}^4, i_x \in \mathcal{U}_x \subseteq \mathbb{R}, i_y \in \mathcal{U}_y \subseteq \mathbb{R}^2$$

As a conservative approach, the constraints on states and inputs are used to define bounds on the disturbance forces using the explicit form of (19) and (20). This leads to compact disturbance sets of the form:

$$F_{dx} \in \mathcal{W}_x \subseteq \mathbb{R}, F_{dy} \in \mathcal{W}_y \subseteq \mathbb{R}^2.$$

Before formulating the proposed MPC, the definition of robust control invariant (RCI) set and robust admissible input (RAI) set are required to enforce state and input constraints. The recursive feasibility of MPC is guaranteed by RCI set as well, see [9], [11] for more details.

Definition 1: **(RCI and RAI set)** Consider a general system $x^+ = f(x,u,w)$, where $x \in \mathcal{X} \subseteq \mathbb{R}^n$, $u \in \mathcal{U} \subseteq \mathbb{R}^m$ and $w \in \mathcal{W} \subseteq \mathbb{R}^q$ are the state, input and disturbance vectors; $\mathcal{X}$, $\mathcal{U}$ and $\mathcal{W}$ are the state, input and disturbance constraint set respectively. The set $\mathcal{R} \subseteq \mathcal{X}$ is a robust control invariant set (RCI) if

$$x(k) \in \mathcal{R}, \exists_{u \in \mathcal{U}} : \\ f(x(k),u(k),w(k)) \in \mathcal{R},\ \forall w \in \mathcal{W}, \forall k \in \mathbb{Z}_{0+}.$$

where $\mathbb{Z}_{0+}$ is the set of non-negative integer number. Furthermore, the set $\mathcal{R}$ is called a control invariant (CI) set if $w = 0$; the set $\mathcal{R}_\infty$ is the maximal robust control invariant set if any $\mathcal{R} \subseteq \mathcal{R}_\infty$. The robust admissible input (RAI) set for $\mathcal{R}$ is $\Theta^u(x) = \{u \in \mathcal{U} | f(x,u,w) \in \mathcal{R}, \forall w \in \mathcal{W}\}$.

With this definition, we require the reference generated by (16) stays in the reference CI set $r(k) \in \mathcal{R}^r_\infty, \forall k \in \mathbb{Z}_{0+}$ during all the process by selecting $u_r(k) \in \Theta^{u_r}(r(k)) \subseteq \mathcal{U}^r$.

Then, to ensure $\left\|x^d - x_m\right\|_\infty \leq \bar{\epsilon}_x$, we start by defining a set of the system and reference states, S^{ξ_x, r_x},

$$\mathcal{S}^{\xi_x,r_x} = \{(\xi_x, r_x) \,|\, \xi_x \in \mathcal{X}_m, r_x \in \mathcal{R}^{r_x}_\infty, \\ \left\|x^d - x_m\right\|_\infty \leq \bar{\epsilon}_x\}. \quad (21)$$

If at any time $k \in \mathbb{Z}_{0+}$ the combined state $(\xi_x(k), r_x(k)) \in \mathcal{S}^{\xi_x,r_x}$, we want the system and reference states stay in $\mathcal{S}^{\xi_x,r_x}$ in the next time instant as well. This requires a RCI set $\mathcal{R}^{\xi_x,r_x} \subseteq \mathcal{S}^{\xi_x,r_x}$ as

$$(\xi_x, r_x) \in \mathcal{R}^{\xi_x,r_x}, \exists_{i_x \in \mathcal{U}_x} : \left(\xi_x^+, r_x^+\right) \in \mathcal{R}^{\xi_x,r_x}, \\ \forall (F_{dx}, a_x) \in (\mathcal{W}_x \times \Theta^{a_x}(r_x)),$$

where $\Theta^{a_x}(r_x)$ is the RAI set for reference CI set $\mathcal{R}^{r_x}$. For system with disturbance, the RCI set is generally not finitely determined. We will use the method proposed in [9] to calculate the $\mathcal{R}^{\xi_x,r_x}$ in finite number of steps.

The reference position trajectory is assumed known N steps ahead, and may be used to establish a reference velocity trajectory. Thus, using the reference $\gamma_x^N(k) = [r_x(k), \cdots, r_x(k+N-1)]^T$, the X-axis MPC solves the following optimisation problem at each time instant:

$$\begin{aligned} U_x^*(k) = &\arg\min_{U_x(k)} \sum_{i=0}^{N-1} \left(Q_x\left(x^d(i) - x_m(i)\right)^2 + R_x i_x^2(i)\right) \\ s.t.\ &\xi_x(i+1) = A_x\xi_x(i) + B_x i_x(i), \\ &x_m(i) = \begin{bmatrix} 1 & 0 \end{bmatrix} \xi_x(i), \\ &x^d(i) = \begin{bmatrix} 1 & 0 \end{bmatrix} r_x(k+i), \\ &\xi_x(i) \in \mathcal{R}^{\xi_x,r_x}(\xi_x, r_x(k+i)),\ \forall i \in \mathbb{Z}_{[0,N-1]} \\ &\xi_x(0) = \xi_x(k), \end{aligned} \quad (22)$$

where Q_x and R_x are the cost function weight on X-axis position error and control input respectively; $U_x(k) = (i_x(0), \cdots, i_x(N-1))$. At each time instant, the optimal control $i_x(k) = i_x^*(0)$ is applied to the plant.

The way of computing RCI set $\mathcal{R}^{\xi_y,r_y}$ is similar to that for $\mathcal{R}^{\xi_x,r_x}$. In order to ensure $\left\|y^d - y_e\right\|_\infty \leq \epsilon_y$, we start with a set S^{ξ_y,r_y}:

$$S^{\xi_y,r_y} = \{(\xi_y, r_y) \,|\, \xi_y \in \mathcal{X}_y, r_y \in \mathcal{R}^{r_y}_\infty, \\ \left\|y^d - y_N - \bar{x}_m\theta + d\right\|_\infty \leq \epsilon_y\}. \quad (23)$$

Since x_m is approximated as a piecewise constant $\bar{x}_m$ over its operating range, for system (20) we need to compute the RCI set $\mathcal{R}^{\xi_y,r_y}$ for each instant of $\bar{x}_m$. Clearly, there is another trade-off in that using finer intervals in $\bar{x}_m$ leads to a better approximation of x_m, but leads to more controller switching and requires more off-line calculation and storage of the RCI sets. The following requirement is imposed for the off-line RCI set calculations:

$$(\xi_y, r_y) \in \mathcal{R}^{\xi_y,r_y}, \exists_{i_y \in \mathcal{U}_y} : \\ \left(A_y(\bar{x}_m)\xi_y + B_y(\bar{x}_m)i_y + E_y(\bar{x}_m)F_{dy}, r_y^+\right) \in \mathcal{R}^{\xi_y,r_y}, \\ \forall (F_{dy}, a_y) \in (\mathcal{W}_y \times \Theta^{a_y}(r_y)),$$

where $\Theta^{a_y}(r_y)$ is the RAI set for reference CI set $\mathcal{R}^{r_y}$.

At time instant k, the predictive controller for controlling y_N and θ solves the on-line optimisation based on reference $\gamma_y^N(k) = [r_y(k), \cdots, r_y(k+N-1)]^T$:

$$\begin{aligned} U_y^*(k) = &\arg\min_{U_y(k)} \sum_{i=0}^{N-1} \left(Q_y\left(y^d(i) - y_e(i)\right)^2 + \|i_y(i)\|^2_{R_y}\right) \\ s.t.\ &\xi_y(i+1) = A_y(\bar{x}_m)\xi_y(i) + B_y(\bar{x}_m)i_y(i), \\ &y_e(i) = \begin{bmatrix} 1 & 0 & \bar{x}_m & 0 \end{bmatrix} \xi_y(i) - d, \\ &y^d(i) = \begin{bmatrix} 1 & 0 \end{bmatrix} r_y(k+i), \\ &\xi_y(i) \in \mathcal{R}^{\xi_y,r_y}(\xi_y, r_y(k+i)),\ \forall i \in \mathbb{Z}_{[0,N-1]} \\ &\xi_y(0) = \xi_y(k), \end{aligned} \quad (24)$$

where $\|i_y(i)\|^2_{R_y} = i_y(i)^T R_y i_y(i)$. At each time instant, the optimal control $i_y(k) = i_y^*(0)$ is applied to the plant. The constraint required in Remark 1 is guaranteed by enforcing the state ξ_y stays in the calculated RCI set.

V. Simulation Results

In this section, the proposed controller is demonstrated on the nonlinear model identified in Section II. The laser head is required to cut a circle with centre at $(0,0)$ and 0.05 m radius. The path includes a straight-line acceleration part to accelerate the Y-axis to maximum velocity.

The maximum speed and acceleration during the cutting process are 0.5 m/s and 5 m/s^2. With a given contouring error bound as 1.5 mm, we choose the X-axis and Y-axis tracking error bound as $\epsilon_x = 1$ mm and $\epsilon_y = 0.5$ mm. The upper bound of rotation angle is chosen as $\theta_{max} = 0.0025$ rad, and this gives $\bar{\epsilon}_x = 0.5$ mm.

For the Y-axis control, the switching LTI model is calculated based on 23 segments for $\bar{x}_m$ from -0.055 m to -0.055 m. The weight in MPC cost function is chosen as $Q_x = Q_y = 10^5$, $R_x = 0.02$ and R_y is chosen a scalar

matrix with multiple 0.02 to put more weight on th tracking errors. The desired and actual contour is shown in Fig. 5. It can be seen that actual contour stays very close to the reference during all the process.

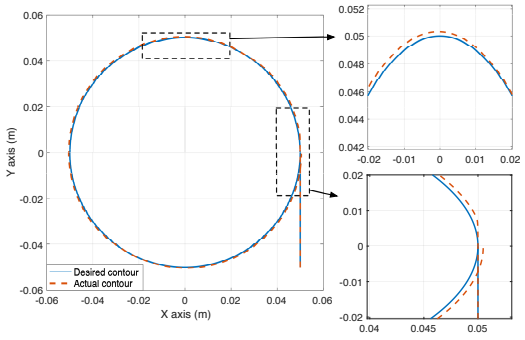

Fig. 5. Desired and actual contour of end effector laser head.

The X-axis tracking error $x^d - x_e$ is shown in Fig. 6. The profile of the rotation angle θ and Y-axis tracking error $y^d - y_e$ are shown in Fig. 7. It is clear the constraints of $\|e_x\|_\infty \leq 1$ mm and $\|e_y\| \leq 0.5$ mm are satisfied.

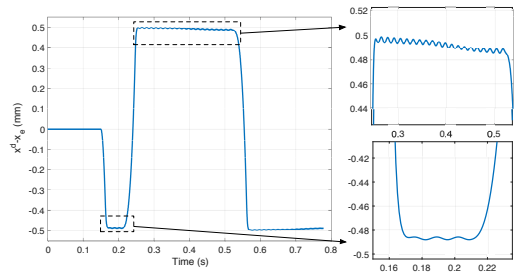

Fig. 6. X-axis tracking error.

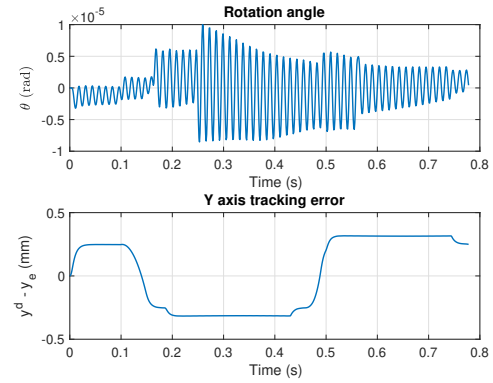

Fig. 7. Rotation angle and Y-axis tracking error.

Since the entire path only consists of straight line and circle. The actual contouring error can be directly calculated and is illustrated in Fig. 8. The maximum contouring error is 0.58 mm, which is below the specified error and is around 1.16% of the circle radius. The simulation results demonstrate the ability of the proposed controller in meeting a specified contouring error requirement.

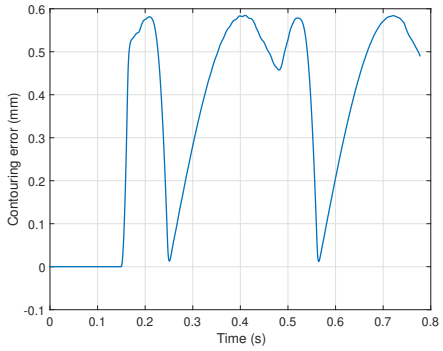

Fig. 8. Actual contouring error during the whole process.

VI. Conclusion and Future Work

A model for a dual drive industrial gantry machine was proposed, and captures twist in the gantry beam that may lead to contour tracking problems. This was used in the design of a new biaxial model predictive controller that can guarantee a given contouring tolerance. Further work will investigate implementation on real machines, with code optimisation for storage and controller execution time considerations; as well as any limitations on the reference trajectories selection in the calculation of the RCI sets used in the controller.

References

[1] S. L. Chen, H. L. Liu, and S. C. Ting, "Contouring control of biaxial systems based on polar coordinates," *IEEE/ASME Trans. Mechatronics*, vol. 7, no. 3, pp. 329–345, 2002.

[2] K. S. Sollmann, M. K. Jouaneh, and D. Lavender, "Dynamic modeling of a two-axis, parallel, H-frame-type XY positioning system," *IEEE/ASME Trans. Mechatronics*, vol. 15, no. 2, pp. 280–290, 2010.

[3] H. K. Park, S. S. Kim, J. M. Park, T. Y. Cho, and D. Hong, "Dynamics of dual-drive servo mechanism," in *IEEE Int. Symp. on Industrial Electronics*, 2001, pp. 1996 –2000.

[4] C. S. Teo, K. K. Tan, S. Y. Lim, S. Huang, and E. B. Tay, "Dynamic modeling and adaptive control of a H-type gantry stage," *Mechatronics*, vol. 17, no. 7, pp. 361–367, 2007.

[5] C. Li, B. Yao, and Q. Wang, "Modeling and Synchronization Control of a Dual Drive Industrial Gantry Stage," *IEEE/ASME Trans. Mechatronics*, vol. 23, no. 6, pp. 2940–2951, 2018.

[6] C. Hu, B. Yao, and Q. Wang, "Coordinated Adaptive Robust Contouring Control of an Industrial Biaxial Precision Gantry With Cogging Force Compensations," *IEEE Trans. Ind. Electron.*, vol. 57, no. 5, pp. 1746–1754, 2010.

[7] B. Yao, C. Hu, and Q. Wang, "An Orthogonal Global Task Coordinate Frame for Contouring Control of Biaxial Systems," *IEEE/ASME Trans. Mechatronics*, vol. 17, no. 4, pp. 622–634, 2012.

[8] F. J. Lin, P. H. Chou, C. S. Chen, and Y. S. Lin, "Three-degree-of-freedom dynamic model-based intelligent nonsingular terminal sliding mode control for a gantry position stage," *IEEE Trans. Fuzzy Syst.*, vol. 20, no. 5, pp. 971–985, 2012.

[9] M. Yuan, C. Manzie, M. Good, I. Shames, F. Keynejad, and T. Robinette, "Bounded Error Tracking Control for Contouring Systems with End Effector Measurements," in *Proc. 20th IEEE Int. Conf. on Industrial Technology*, 2019, pp. 66–71.

[10] L. Wang, H. Liu, L. Yang, J. Zhang, W. Zhao, and B. Lu, "The effect of axis coupling on machine tool dynamics determined by tool deviation," *Int. J. of Machine Tools and Manufacture*, vol. 88, pp. 71–81, 2015.

[11] S. Di Cairano and F. Borrelli, "Reference Tracking With Guaranteed Error Bound for Constrained Linear Systems," *IEEE Trans. Autom. Control*, vol. 61, no. 8, pp. 2245–2250, 2016.